https://doi.org/10.5194/egusphere-2025-4174
Preprint. Discussion started: 14 October 2025

Passive acoustic monitoring from profiling floats as a pathway to scalable autonomous observations of global surface wind

Louise Delaigue[1], Pierre Cauchy[2], Dorian Cazau[3], Julien Bonnel[4], Sara Pensieri[5], Roberto Bozzano[5], Anatole Gros-Martial[6], Christophe Schaeffer[7], Arnaud David[7], Paco Stil[1], Antoine Poteau[1], Catherine Schmechtig[8], Edouard Leymarie[1] and Hervé Claustre[1]

[1]Sorbonne Université, CNRS, Laboratoire d'Océanographie de Villefranche, LOV, 06230 Villefranche-sur-Mer, France

[2]Institut des sciences de la mer (ISMER), Université du Québec à Rimouski (UQAR), Rimouski, Québec, Canada

[3]ENSTA, Lab-STICC, UMR CNRS 6285, Brest, France

[4]Marine Physical Laboratory, Scripps Institution of Oceanography, University of California San Diego, La Jolla, CA, 92093, USA

[5]Institute for the Study of Anthropic Impact and Sustainability in the Marine Environment (IAS), Consiglio Nazionale delle Ricerche (CNR), Genoa, Italy

[6]Centre d'Études Biologiques de Chizé, CNRS, Villiers-en-bois, France

[7]NKE Instrumentation, Hennebont, France

[8]OSU Ecce Terra, UAR 3455, CNRS, Sorbonne Université, Paris Cedex, France

Correspondence to: Louise Delaigue (louise.delaigue@imev-mer.fr)

Abstract. Wind forcing plays a pivotal role in driving upper-ocean physical and biogeochemical processes, yet direct wind observations remain sparse in many regions of the global ocean. While passive acoustic techniques have been used to estimate wind speed from moored and mobile platforms, their application to profiling floats has been demonstrated only in limited cases and remains largely unexplored. Here, we report on the first deployment of a profiling float equipped with a passive acoustic sensor, aimed at detecting wind-driven surface signals from depth. The float was deployed in the northwestern Mediterranean Sea near the DYFAMED meteorological buoy from February to April 2025, operating at parking depths of 500–1000 m. We demonstrate that wind speed can be successfully retrieved from subsurface ambient noise using established acoustic algorithms, with float-derived estimates showing good agreement with collocated surface observations from the DYFAMED buoy. To evaluate the potential for broader application, we simulate a remote deployment scenario by refitting the acoustic model of Nystuen et al. (2015) using ERA5 reanalysis as a proxy for surface wind. Refitting the model to ERA5 data demonstrates that the float–acoustic–wind relationship is generalizable in moderate conditions, but high-wind regimes remain systematically biased—especially above 10 m s^{-1}. Finally, we apply a residual learning framework to correct these estimates using a limited subset of DYFAMED wind data, simulating conditions where only brief surface observations—such as those from a ship during float deployment—are available. The corrected wind time series achieved a 37% reduction in RMSE and improved the coefficient of determination (R^2) from 0.85 to 0.91, demonstrating the effectiveness of combining reanalysis with sparse in-situ fitting. This framework enables the retrieval of fine-scale wind variability not captured by reanalysis alone, supporting a scalable strategy for float-

https://doi.org/10.5194/egusphere-2025-4174
Preprint. Discussion started: 14 October 2025

based wind monitoring in data-sparse ocean regions—with important implications for quantifying air–sea exchanges, improving biogeochemical flux estimates, and advancing global climate observations.

1 Introduction

Wind plays a fundamental role in driving ocean dynamics, air–sea fluxes of gases and governing biological productivity and climate-related biogeochemical processes (Wanninkhof, 2014; McGillicuddy, 2016). Recent modelling studies emphasize that wind-driven ocean circulation significantly influences regional climate trends, such as the North Atlantic Warming Hole phenomenon (McMonigal et al., 2025). Despite its critical importance, accurately quantifying oceanic wind variability remains challenging, particularly in remote and undersampled regions such as the Southern Ocean, where satellite retrievals are limited by coarse resolution, signal degradation from storms, heavy cloud cover, and sea ice (Bentamy et al., 2003; Chelton et al., 2007; Verhoef et al., 2012). Consequently, observational gaps persist, affecting our understanding of critical processes like air-sea carbon exchange during storm events (Carranza et al., 2024).

Traditionally, oceanic wind observations have relied heavily on satellite scatterometry and surface-based platforms, including meteorological buoys. While scatterometers provide near-global wind observations, their effectiveness diminishes significantly under stormy conditions, heavy precipitation, and seasonal ice coverage, limiting the accuracy and temporal resolution required to capture highly dynamic atmospheric conditions at high latitudes (Chelton et al., 2007; Verhoef et al., 2012). Surface platforms, although providing high-resolution data, suffer from spatial limitations and high deployment and maintenance costs.

An alternative method with substantial promise involves using passive acoustic sensing of underwater ambient noise generated by surface wind stress and wave-breaking activities. The relationship between wind speed and high-frequency ambient noise (1–20 kHz) has been extensively validated through theoretical and empirical studies (Vagle et al., 1990; Farmer et al., 1998; Oguz and Prosperetti, 1990). These foundational studies demonstrated that air bubble entrainment due to wave breaking, and raindrop impacts produces distinctive acoustic signatures, offering a robust proxy for surface meteorological conditions. This approach builds on the Weather Observations Through Ambient Noise (WOTAN) framework, formally introduced by Vagle et al. (1990), which directly links wind-driven surface processes to characteristic underwater acoustic signatures. The WOTAN methodology has since been successfully implemented in dedicated instruments such as the Passive Acoustic Listener (PAL), enabling autonomous and continuous monitoring of wind and rainfall from subsurface acoustic recordings (Nystuen et al., 2001). Building upon this foundation, Ma et al. (2005) developed a semi-empirical acoustic model capable of discriminating between wind-induced and rain-induced ambient noise features, thereby enabling reliable estimation of wind speeds from subsurface recordings. Subsequent studies extended these methods to drifting and

https://doi.org/10.5194/egusphere-2025-4174
Preprint. Discussion started: 14 October 2025

subsurface platforms, validating the acoustic–wind relationship across varied conditions (Ma and Nystuen, 2005; Nystuen et al., 2015; Pensieri et al., 2015).

Advancements in passive acoustic sensing technology have enabled the integration of acoustic sensors onto autonomous oceanographic platforms, including underwater gliders (Cazau et al., 2018; Cauchy et al., 2018) and profiling floats equipped with PAL sensors (Riser et al., 2008; Yang et al., 2015; Yang et al., 2016; Ma et al., 2023). Such developments are especially valuable in remote environments, where traditional in-situ measurements remain limited. For example, Menze et al. (2012) provided early evidence of wind-dependent acoustic noise regimes in the Weddell Sea, while Cazau et al. (2017) and Gros-Martial et al. (2025) extended these methods by using biologged southern elephant seals, demonstrating the feasibility of estimating wind speed from passive acoustic recordings in the polar frontal zone. Beyond atmospheric sensing, acoustic-equipped profiling floats have also proven valuable for a broader range of geophysical and ecological applications, including detection and classification of marine mammal vocalizations (Matsumoto et al., 2013; Baumgartner and Bonnel, 2022), monitoring of hydroacoustic earthquake signals and ambient ocean noise (Pipatprathanporn and Simons, 2022), and observing the presence of deep-diving cetaceans (Matsumoto et al., 2013; Fregosi et al., 2020).

Despite these advancements, integration of passive acoustic sensors onto modern biogeochemical (BGC)-Argo floats remains underexplored. BGC-Argo floats represent a transformative technology in ocean observing, providing extensive datasets of critical oceanic parameters including oxygen, nitrate, chlorophyll, pH, and downwelling irradiance (Johnson and Claustre, 2016; Claustre et al., 2020). These autonomous platforms have significantly improved our understanding of seasonal and interannual variability in nutrient dynamics (Johnson et al., 2010), primary productivity (D'ortenzio et al., 2020), ocean acidification (Williams et al., 2017), and carbon sequestration (Gray et al., 2018). Integrating acoustic wind-sensing capabilities with BGC-Argo floats thus offers a unique opportunity to simultaneously capture critical atmospheric forcing parameters alongside biogeochemical observations.

Recent technological developments, including miniaturized, low-power acoustic sensors optimised for integration into autonomous platforms, now enable passive acoustic wind estimation with minimal impact on float energy budgets and data transmission constraints (Baumgartner et al., 2017). These advancements facilitate real-time onboard processing and transmission of acoustic-derived environmental variables via satellite, thus overcoming historical barriers associated with power consumption and data management. The integration of acoustic sensors into BGC-Argo floats thereby holds promise for closing significant observational gaps, particularly in undersampled regions such as the Southern Ocean.

Furthermore, the broader international scientific community has recognized the value of passive acoustic sensing within global ocean observing frameworks. The Ocean Sound Essential Ocean Variable (EOV), coordinated by the International Quiet Ocean Experiment

https://doi.org/10.5194/egusphere-2025-4174
Preprint. Discussion started: 14 October 2025

(IQOE) and endorsed by the Global Ocean Observing System (GOOS), specifically identifies profiling floats as ideal platforms for scalable, distributed acoustic monitoring. This aligns with current efforts to enhance autonomous ocean observing systems through multidisciplinary sensor integration.

In this study, we present the first deployment of a profiling float equipped with a passive acoustic sensor designed explicitly for wind speed estimation from subsurface ambient noise. Deployed in the northwestern Mediterranean Sea, near the DYFAMED meteorological buoy, this float serves as a proof-of-concept demonstration by integrating advanced acoustic sensing with simultaneous biogeochemical measurements. Our main objective is to assess the feasibility and precision of acoustic-based wind retrieval methods by applying and refining established empirical algorithms tailored specifically to the acoustic characteristics of the profiling platform. We validate float-derived wind estimates using collocated observations from the DYFAMED buoy and the ERA5 atmospheric reanalysis dataset, highlighting both the strengths and limitations of existing reference products. Finally, we propose a practical framework whereby acoustic observations from the float can be effectively combined with reanalysis data to enhance the accuracy of wind estimates in remote, data-sparse regions. Through this approach, we demonstrate the potential of acoustic-equipped profiling floats to serve as scalable, autonomous platforms within global ocean observing networks and capable of closing critical observational gaps, improving quantification of air–sea exchanges, and enriching our understanding of oceanic and climatic processes.

https://doi.org/10.5194/egusphere-2025-4174
Preprint. Discussion started: 14 October 2025

2 Materials and Methods

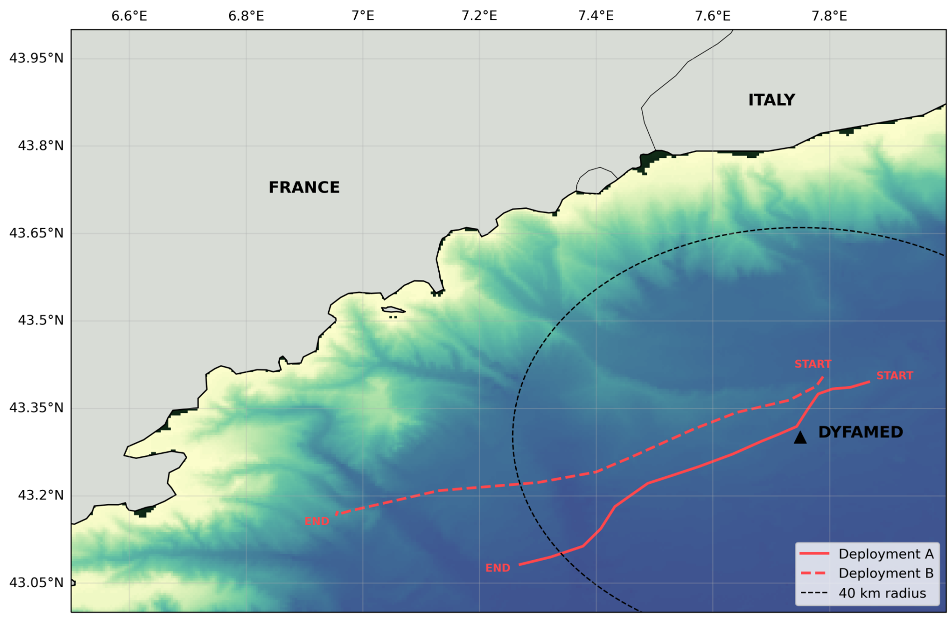

Figure 1. Float trajectories during sea trials conducted in the Ligurian Sea in February and March 2025. Deployment A (solid line) and Deployment B (dashed line) are shown along with a concentric dashed circle (40 km radius) centred on the DYFAMED station. The 40 km radius was used to spatially filter float data for refitting and validation of wind estimates at DYFAMED, as described in Cauchy et al. (2018).

2.1 Study area and DYFAMED weather station

The acoustic wind sensing trial was conducted in the Ligurian Sea, a sub-basin of the northwestern Mediterranean, in proximity to the DYFAMED (DYnamique des Flux Atmosphériques en MEDiterranée) oceanographic time series station (Fig. 1). DYFAMED (43.42°N, 7.87°E) has served as a key reference site for air–sea exchange, upper ocean dynamics, and biogeochemical cycling since the early 1990s. The station is equipped with continuous meteorological and oceanographic monitoring, including high-quality wind speed and direction measurements from a surface buoy maintained by Météo-France. These data are reported at hourly resolution, following WMO (World Meteorological Organization) standards, and include wind parameters, along with air temperature, pressure, humidity, and sea state. During the study period, wind speeds at DYFAMED ranged from 0.5 to 16.1 m s^{-1}, with a mean of 6.8 m s^{-1} and a measurement precision of one decimal place.

https://doi.org/10.5194/egusphere-2025-4174
Preprint. Discussion started: 14 October 2025

2.2 Acoustic sensor integration

The float used in this study was equipped with a passive acoustic module jointly developed by NKE and ABYSsens in collaboration with LOV. This module was specifically designed for integration into the PROVOR CTS5 BGC-Argo platform, with the aim of minimizing power consumption and data volume while remaining compatible with the operational constraints of the BGC-Argo program.

The module consists of two main parts enclosed in a dedicated external housing: 1) a low-noise HTI-96-Min hydrophone (sensitivity: −165 dB re 1 V/μPa; frequency range: 2 Hz–30 kHz), mounted externally to capture pressure fluctuations, and 2) an ABYSsens acquisition board, which conditions, digitizes, and processes the signal.

The acquisition system operates in a low-power pulsed mode (220 mW) with a sampling frequency up to 62.5 kHz and 24-bit resolution. To limit power usage and transmission needs, raw acoustic signals are not stored. Instead, the sensor performs direct onboard integration into 23 third-octave bands, spanning from 63 Hz to 25 kHz with a variable integration time (see Table 1). Higher-frequency bands (e.g., 3.15–25 kHz) used shorter integration times (50 ms), while low-frequency bands used longer windows (up to 500 ms).

Frequency band range	**Integration time**
63, 100, **125** and 160 Hz	500 ms
400, 500 and 630 Hz	250 ms
800 Hz, **1**, 1.25, 1.6, **2** and 2.5 kHz	100 ms
3.15, 4, **5**, 6.3, **8**, 10, **12.5**, 16, **20** and 25 kHz	50 ms

Table 1. Integration times applied to third-octave bands during acoustic signal processing, varying by frequency range to balance energy and spectral accuracy. In bold and underlined, the bands transmitted in the "9 bands" float configuration.

The acoustic unit is mounted on the upper section of the float chassis and is configured to operate exclusively during the parking phase (500–1000 m depth). During this phase, the float drifts with only routine background measurements (e.g., pressure, CTD), and acoustic acquisition is automatically suspended whenever noisy operations such as ballast pumping or CTD sampling occur, thereby avoiding contamination from self-noise.

The float system allows for flexible and modifiable configuration via satellite: the user can define the number of bands transmitted (23, 9, or a compact onboard estimate of wind/rain),

https://doi.org/10.5194/egusphere-2025-4174
Preprint. Discussion started: 14 October 2025

the acquisition interval (typically 5–15 minutes), and the number of acoustic samples averaged per measurement. In this study, we used a 5-minute interval with 10 averaged acquisitions per measurement (each acquisition is a spectral estimation using the integration times defined in Table 1).

The telemetry and energy impact of adding an acoustic sensor to a 6-variable biogeochemical float was evaluated by using the programming interface provided by NKE. The estimated reduction in the number of cycles varies from 18% for acquisition every 5 minutes to 7% for acquisition every 15 minutes during the whole parking drift of a 10-day Argo cycle and with 5 averaged acquisitions per acoustic measurement. The data volume increase depends on the transmission format: from ~9% for onboard wind–rain estimates (15-min period) to ~85% for a full 23-band spectrum (5-min period). A 9-band spectrum every 15 minutes—a likely recommended setup—adds ~16%. These overheads remain within the platform's capacity, confirming compatibility with concurrent BGC measurements.

Each sensor output transmitted by the float corresponds to the Third Octave Level (TOL), i.e., the sound pressure level integrated over a third-octave band, expressed in dB re 1 µPa. These TOLs represent the float's primary spectral product and are used as input to the wind speed retrieval models. The amplitude resolution of the transmitted data is 0.2 or 0.5 dB, with a dynamic range up to 127 dB. This discretisation arises because the data are transmitted as integers to save bandwidth, which requires selecting a resolution step.

2.3 Depth correction and spectral normalization

To account for the attenuation of surface-generated noise with depth, a correction was applied to all acoustic measurements (Fig. 2). In this study, the correction term was calculated from the first temperature–salinity profile (Fig. 2a-b) and applied throughout the deployment, as the float remained in relatively stable hydrographic conditions (Fig. 2c). For long-term or basin-scale missions, however, this coefficient would need to be recomputed for each profile, since temperature and salinity variability along the float trajectory can significantly affect sound propagation.

Following Cauchy et al. (2018), the correction takes the form:

$$\mathrm{TOL}_0(\mathrm{f}) = \mathrm{TOL}(\mathrm{h},\mathrm{f}) + \beta(\mathrm{h},\mathrm{f}) \quad \text{(1a)},$$

$$\text{where } \beta(\mathrm{h},\mathrm{f}) = -10\log\left\{2\int_0^{\infty}\left[\frac{r\, sin^2\theta_{r,h}\, e^{-\alpha_f\, l_{r,h}}}{l^2_{r,h}}\right]\mathrm{dr}\right\} \quad \text{(1b)},$$

https://doi.org/10.5194/egusphere-2025-4174
Preprint. Discussion started: 14 October 2025

with TOL(h, f) as the raw TOL measurement from the profiling float, h as the sensor depth, f the centre frequency of the band, r the horizontal distance from a surface noise source to the point vertically above the sensor, l the total pathlength between source and receiver (accounting for depth and refraction), including refraction effects, θ the angle between the emitted acoustic ray and the horizontal axis, and α the frequency-dependent attenuation coefficient for bubble-free water. The integral considers contributions from all surface-generated acoustic sources over the sea surface, assuming radial symmetry, and accounts for geometric spreading, frequency-dependent absorption, and angle-dependent energy emission along each path. This correction was originally derived for third-octave levels and is directly applicable here, as the float outputs TOLs at fixed centre frequencies.

Then, depth-corrected third-octave levels (in dB re 1 μPa) were converted to spectral density levels (dB re 1 μPa/Hz) by normalising to the bandwidth of each band. This step ensures consistency across frequencies and comparability with model spectra. In future deployments, this spectral correction will be applied directly onboard the float.

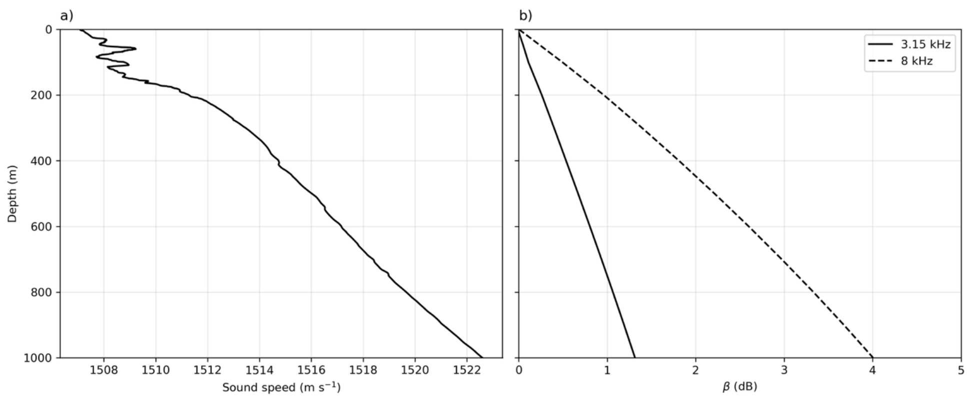

Figure 2. a) Sound speed profile used to derive the b) depth correction term β(h, f) as a function of depth, following the formulation of Cauchy et al. (2018). The correction accounts for the attenuation of wind-generated surface noise with increasing sensor depth and was applied prior to wind speed estimation. Here, β is shown at 3.15 kHz and 8 kHz.

https://doi.org/10.5194/egusphere-2025-4174
Preprint. Discussion started: 14 October 2025

2.4 Profiling float deployments

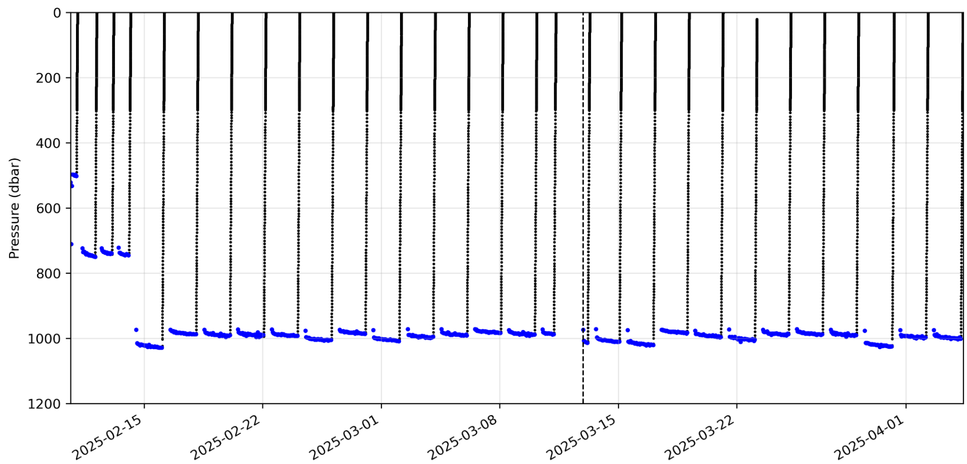

Figure 3. Vertical profiles from the acoustic-equipped profiling float deployed near DYFAMED between February and April 2025. Blue points indicate times when passive acoustic data were successfully recorded. The vertical dashed line marks the transition between Deployment A and Deployment B.

Two deployments of an acoustic-equipped float (PROVOR CTS5) were carried out near DYFAMED between February and April 2025 (Fig. 1). Deployment A lasted 30 days, from 10 February to 11 March, and Deployment B continued for 24 days starting on 12 March and remained active until 4 April. The float operated in park-and-profile mode at three parking depths (500, 700, and 1000 m; Fig. 2), collecting biogeochemical data during ascent and passive acoustic data exclusively during the parking phases to minimize self-generated noise.

While Riser et al. (2008) previously demonstrated the feasibility of acoustic wind sensing from Argo floats, their system transmitted only pre-processed wind estimates derived onboard using a simplified version of the algorithm by Nystuen et al. (2015), without retaining or transmitting spectral band data. This limited the possibility of reanalysis or applying alternative processing schemes. In contrast, the floats used in this study recorded and transmitted full third-octave band spectra, enabling detailed post-processing and algorithm refinement tailored to the float's specific acoustic characteristics.

2.5 Transient and anthropogenic noise mitigation

Transient noise (i.e. episodic non-wind-related events) was mitigated by removing values exceeding the 99th percentile within a ±1.5-hour window centred around each matched timestamp. While this approach risks excluding some high-wind events, we verified that

https://doi.org/10.5194/egusphere-2025-4174
Preprint. Discussion started: 14 October 2025

extreme wind episodes typically span durations longer than a few hours, minimizing the chance of misclassification (see Fig. 8).

To further reduce short-term variability and emphasize quasi-stationary wind-driven acoustic patterns, we applied a 3-hour rolling mean to each frequency band. This choice reflects a compromise between noise reduction and temporal resolution: the smoothing is sufficient to stabilize wind estimates in the presence of submesoscale variability and intermittent noise, yet long enough to preserve multi-hour wind events of interest. While this approach may attenuate very brief fluctuations, our inspection of the time series suggests that the smoothing is sufficient to suppress noise while retaining multi-hour processes of interest (eg., air–sea fluxes). Alternative strategies, such as post-processing the wind speed estimates rather than the spectral bands, could be explored in future deployments if finer-scale variability is a priority.

To mitigate anthropogenic noise contamination, Automatic Identification System (AIS) ship tracking data were used to identify vessel presence within a 10 km radius and ±30 minutes of each float timestamp. Acoustic observations were flagged as potentially contaminated if they coincided with ship presence *and* showed anomalous deviations—defined as float-derived wind speed differing from the DYFAMED buoy estimate by more than the root mean square error (RMSE) observed under uncontaminated conditions. While this introduces a partial dependence on external wind reference data, the combined AIS+anomaly criterion reduces false positives and avoids relying solely on model–sensor differences for data exclusion. Data flagged as contaminated were excluded from further analysis.

https://doi.org/10.5194/egusphere-2025-4174
Preprint. Discussion started: 14 October 2025

2.6 Application of established acoustic models

Model	Input units	Wind frequency band (kHz)	Wind retrieval frequency (kHz)
Vagle et al. (1990)	dB re 1 µPa²/Hz	7.1–8.9	8
Nystuen et al. (2015)	dB re 1 µPa²/Hz	7.1–8.9	8
Pensieri et al. (2015)	dB re 1 µPa²/Hz	7.1–8.9	8
Cauchy et al. (2018)	dB re 1 µPa	2.8–3.55	3.15

Table 2. Summary of acoustic wind speed estimation models and their input requirements. Input units refer to the spectral level units used in model calibration. Central frequency indicates the nominal retrieval frequency, and the third-octave band column specifies the corresponding bandwidth. All models were calibrated and validated against standard 10-m wind speed.

Empirical models have long been used to estimate surface wind speed from underwater ambient noise, exploiting the link between wind-driven bubble formation and acoustic energy in the 1–20 kHz band. These models typically relate surface wind speed U to the sound pressure level L_f measured in selected frequency bands. While many models use third-octave bands, others rely on custom-defined or narrowband frequencies, often with variable bandwidths (e.g., 16% of the centre frequency in Vagle et al., 1990).

We applied four established wind retrieval models spanning a range of functional forms—cubic, two-regime linear–quadratic, composite, and two-regime log–linear. All wind models were applied using acoustic levels consistent with their original formulations (Table 2). This diversity allowed us to assess sensitivity to model structure and evaluate performance under float-specific conditions. Each model was first implemented using its published coefficients to generate wind speed estimates from float acoustic data, and the results were evaluated against collocated meteorological observations (Fig. 4). Subsequently, the parameters of each model were refitted using collocated float acoustic and wind data from the DYFAMED meteorological buoy (Figs. 4 and 5; see Table 1 in Supplementary Material), which provides

https://doi.org/10.5194/egusphere-2025-4174
Preprint. Discussion started: 14 October 2025

hourly 10-meter wind speed. Model refitting was performed using nonlinear least-squares optimization (Table 3). Wind records from DYFAMED were matched to float measurements by nearest timestamp.

Following the spatial filtering approach of Cauchy et al. (2018), only float data within 40 km of DYFAMED were retained for refitting and validation (Fig. 1). This threshold corresponds to the estimated confidence radius around the DYFAMED meteorological buoy, within which wind speed measurements show high spatial coherence ($R = 0.86$, $RMSE = 2.5$ m s^{-1}) when compared to the AROME-WMED atmospheric model (Rainaud et al., 2016). The updated coefficients were then used to generate wind estimates over the full float dataset. While this spatial proximity improves wind representativeness, it does not account for variations in wind fetch, a parameter known to influence ambient noise generation, particularly through wave and bubble field development (e.g., Prawirasasra et al., 2024).

These four models were selected to represent a range of analytical formulations commonly used in acoustic wind retrievals. They all use frequency bands where wind-driven bubble noise typically dominates the local ambient sound field, with reduced interference from low-frequency sources such as distant shipping. Our aim was not to exhaust all available models, but rather to evaluate a representative subset under consistent float-specific conditions, emphasizing the effect of model structure and local fitting.

The specifications and key features of each model are summarized in Table 2 for reference. For all models and validation steps throughout the rest of Methods section, wind speed refers to the standard 10-meter wind speed, consistent with both the ERA5 reanalysis product and the DYFAMED buoy observations used for calibration and evaluation.

The first model, from Vagle et al. (1990), was derived from moored hydrophone data in the North Atlantic and relates wind speed to high-frequency noise at 8 kHz using a cubic formulation:

$$U_{\mathrm{Vagle\ 1990}} = 10^{(\frac{-38.70 + \sqrt{-38.70^2 - 4.7 \cdot 38 \cdot (SPL_{8kHz} - 21.69)}}{-7.38 \cdot 2}} \quad (2).$$

Next, we applied the cubic model from Nystuen et al. (2015), developed using long-term acoustic records from fixed hydrophones in both the Pacific and Atlantic. This model targets wind-generated noise at 8 kHz and includes band-specific criteria to distinguish wind contributions from other sources such as rain and shipping (Table 2).

$$U_{\mathrm{Nystuen\ 2015}} = 0.0005 \cdot {SPL_{8kHz}}^3 - 0.0310 \cdot {SPL_{8kHz}}^2 + 0.4904 \cdot SPL_{8kHz} + 2.0871 \quad (3).$$

https://doi.org/10.5194/egusphere-2025-4174
Preprint. Discussion started: 14 October 2025

We then tested the two-regime linear–quadratic model from Pensieri et al. (2015) at 8 kHz, developed using moored hydrophone data from the Ligurian Sea, near our study area. Calibrated for Mediterranean conditions, the model relates wind speed to ambient noise levels at the 8 kHz band, applying distinct linear and quadratic fits across low- and high-noise regimes. Notably, the transition between regimes is defined at 38 dB, corresponding to a wind speed of 2.39 m s^{-1} in their framework. However, it is important to note that the threshold separating high and low regimes is not standardized across the literature and may vary between studies.

$$U_{\text{Pensieri 2015}} = \begin{cases} 0.044642 \cdot \text{SPL}_{8\text{kHz}}{}^{2} - 3.2917 \cdot \text{SPL}_{8\text{kHz}} + 63.016 \\ 0.1458 \cdot \text{SPL}_{8\text{kHz}} - 3.146, \text{for } \text{SPL}_{8\text{kHz}} < 38 \text{ dB} \end{cases} \quad (4).$$

Finally, we included the two-regime log–linear model from Cauchy et al. (2018), developed using acoustic data from a glider operating in the western Mediterranean. Designed for mobile platforms, the model relates wind speed to third-octave noise levels centred at 3 kHz. The model uses distinct logarithmic and linear fits across two noise regimes.

This choice of 3 kHz, instead of the more commonly used 8 kHz, was based on empirical observations showing greater dynamic range and lower variance in this band, which may reflect sensor-specific factors or the sensor's mounting configuration on the glider (Cauchy et al., 2018). The relationship goes as:

$$U_{\text{Cauchy 2018}} = \begin{cases} \dfrac{1}{0.4 \cdot 10^{4}} \cdot \left(10^{\frac{\text{SPL}_{3\text{kHz}} - S_{\text{off}}}{20}} + 0.2 \cdot 10^{4}\right) \\ \dfrac{1}{1.6 \cdot 10^{4}} \cdot \left(10^{\frac{\text{SPL}_{3\text{kHz}} - S_{\text{off}}}{20}} + 12.5 \cdot 10^{4}\right) \text{for } U > 10 \text{ m s}^{-1} \end{cases} \quad (5).$$

The wind retrieval relationship is modelled using a two-regime log-linear function. The transition between regimes occurs at wind speeds of approximately 10–11 m s^{-1}, established empirically. To represent this switching behaviour, a relative threshold level is introduced, expressed as SPL – S_{off}, where S_{off} denotes the sea-state 0 noise reference. This formulation highlights when wind-driven noise becomes dominant relative to the reference background noise.

2.7 Simulated wind estimation using reanalysis and residual learning

To evaluate the ability of float-derived acoustic measurements to estimate surface wind speed in regions without direct atmospheric observations, we used wind data from the ERA5 atmospheric reanalysis produced by the European Centre for Medium-Range Weather

https://doi.org/10.5194/egusphere-2025-4174
Preprint. Discussion started: 14 October 2025

Forecasts (ECMWF; Bell et al., 2021). ERA5 provides global wind fields on a 0.25° × 0.25° spatial grid with hourly temporal resolution, offering a consistent and widely used reference for surface atmospheric conditions.

Hourly ERA5 data were retrieved for the period spanning the float deployments, from 10 February to 31 March 2025. Specifically, we extracted the 10 m zonal (u_{10}^2) and meridional (v_{10}^2) wind components from the grid cell containing the float's position. Wind speed (U) was then computed as:

$$U = \sqrt{u_{10}^2 + v_{10}^2} \quad (6).$$

These values were time-matched to float and DYFAMED measurements using the nearest available ERA5 hour.

Using ERA5 wind speeds as a reference, we refitted the empirical model from Nystuen et al. (2015; 3) to float-measured Sound Pressure Level (SPL) at 8 kHz, producing a new set of coefficients tailored to the float deployment. This produced a first-pass wind estimate derived from float acoustics alone, calibrated to ERA5 rather than to DYFAMED in-situ observations. This approach simulates a scenario in which a profiling float is deployed in a remote region lacking surface wind measurements, and reanalysis products are used to train or tune the acoustic model.

To improve the accuracy of this ERA5-calibrated estimate, we developed a residual learning framework that uses limited collocated DYFAMED in-situ observations to correct systematic errors. This training set, consisting of observations within 40 km, represents approximately 40% of the full dataset. This setup was designed to simulate a realistic scenario where ship-based wind measurements are available in proximity to a float deployment. Specifically, we used wind speed measurements from the DYFAMED buoy to model residual differences between the ERA5-based acoustic prediction and true surface conditions. A feature matrix was constructed including SPL at 8 kHz, ERA5 wind speed (10-meter), normalized time (deployment day), and the acoustic model prediction wind speed from Nystuen et al. (2015; Eq. 3). Residuals relative to DYFAMED wind speed were modelled using XGBoost regression, a gradient boosting machine learning algorithm based on gradient-boosted decision trees and known for its high predictive performance and ability to handle non-linear relationships and interactions between features (Chen and Guestrin, 2016).

To estimate prediction uncertainty, we applied bootstrapping at two levels. For the ERA5-calibrated acoustic estimate, we generated 100 bootstrap samples by resampling the float dataset with replacement and perturbing the ERA5 wind input using its reported uncertainty (standard deviation $\sigma = 1.5$ m s^{-1}; Bell et al., 2021). The empirical model was re-fitted for each bootstrap, and the resulting ensemble of predictions was used to compute the standard deviation

https://doi.org/10.5194/egusphere-2025-4174
Preprint. Discussion started: 14 October 2025

at each time point. This approach captures both the impact of ERA5 input uncertainty and variability in the fitted model parameters.

For the ML-corrected wind speed, we trained an ensemble of 100 XGBoost models on bootstrapped subsets of the training data. During both training and prediction, Gaussian noise (mean = 0, σ = 1.5 m s^{-1}) was added to the ERA5 wind feature to simulate observational uncertainty. The Gaussian assumption provides a tractable way to propagate uncertainty through the learning framework and is commonly used in ensemble perturbation methods when only first- and second-moment statistics are available. While the true distribution of ERA5 errors may deviate from normality, the central limit tendency of aggregated atmospheric errors makes the Gaussian approximation a reasonable first-order choice. Importantly, this approach ensures that the output uncertainty reflects both the variability of the fitted ML model and the stated input uncertainty, though future work could refine the noise model if detailed error distributions become available. Final corrected wind speeds were computed by summing the Nystuen et al. (2015) ensemble-mean prediction with the ensemble-mean residual. Uncertainty bounds were defined as $\pm 1\sigma$, combining variability across the XGBoost ensemble with ERA5 input uncertainty in quadrature. Uncertainty for the ML-corrected estimate reflects the variability of the residual model and ERA5 input uncertainty but does not propagate the bootstrap spread of the underlying Nystuen fit, which we report separately.

This method demonstrates how passive acoustic observations from profiling floats can be combined with global reanalysis products and limited in-situ data to improve local wind speed estimates, simulating the upscaling of BGC-Argo float deployments in remote ocean regions lacking direct wind speed estimates.

https://doi.org/10.5194/egusphere-2025-4174
Preprint. Discussion started: 14 October 2025

3 Results and Discussion

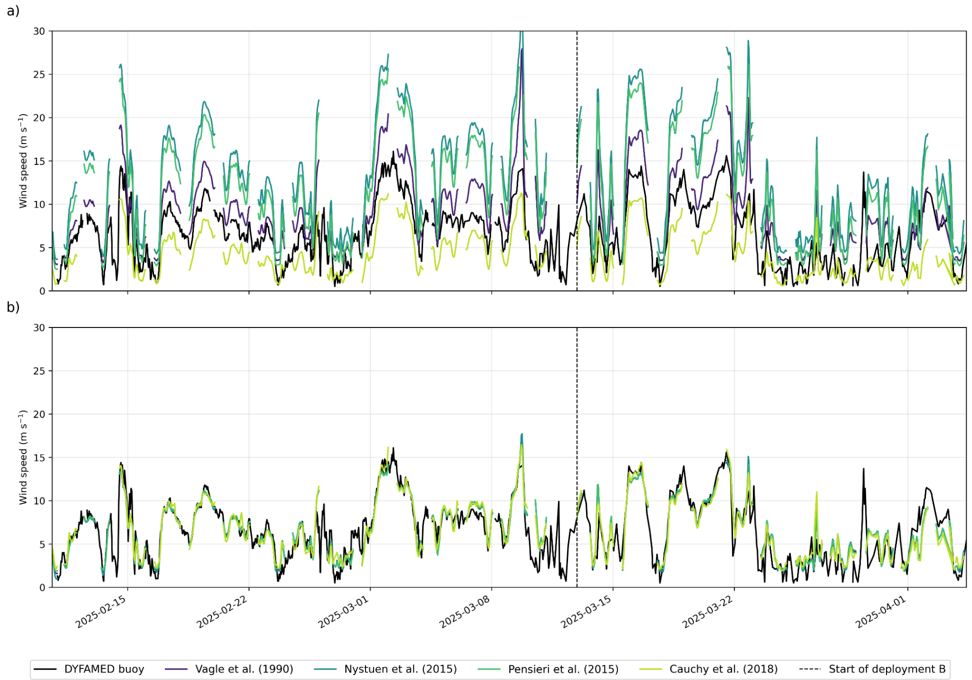

Figure 4. Comparison of unoptimized (top) and optimised (bottom) wind speed models against DYFAMED buoy observations. Each subplot shows modelled wind speed estimates from four literature models (Vagle et al., 1990; Nystuen et al., 2015; Pensieri et al., 2015; Cauchy et al., 2018) compared with collocated buoy wind data (black line). The unoptimized models a) use original published coefficients, while the optimised models b) are re-fitted using data within 40 km of the DYFAMED site. The dashed vertical line indicates the start of deployment B.

https://doi.org/10.5194/egusphere-2025-4174
Preprint. Discussion started: 14 October 2025

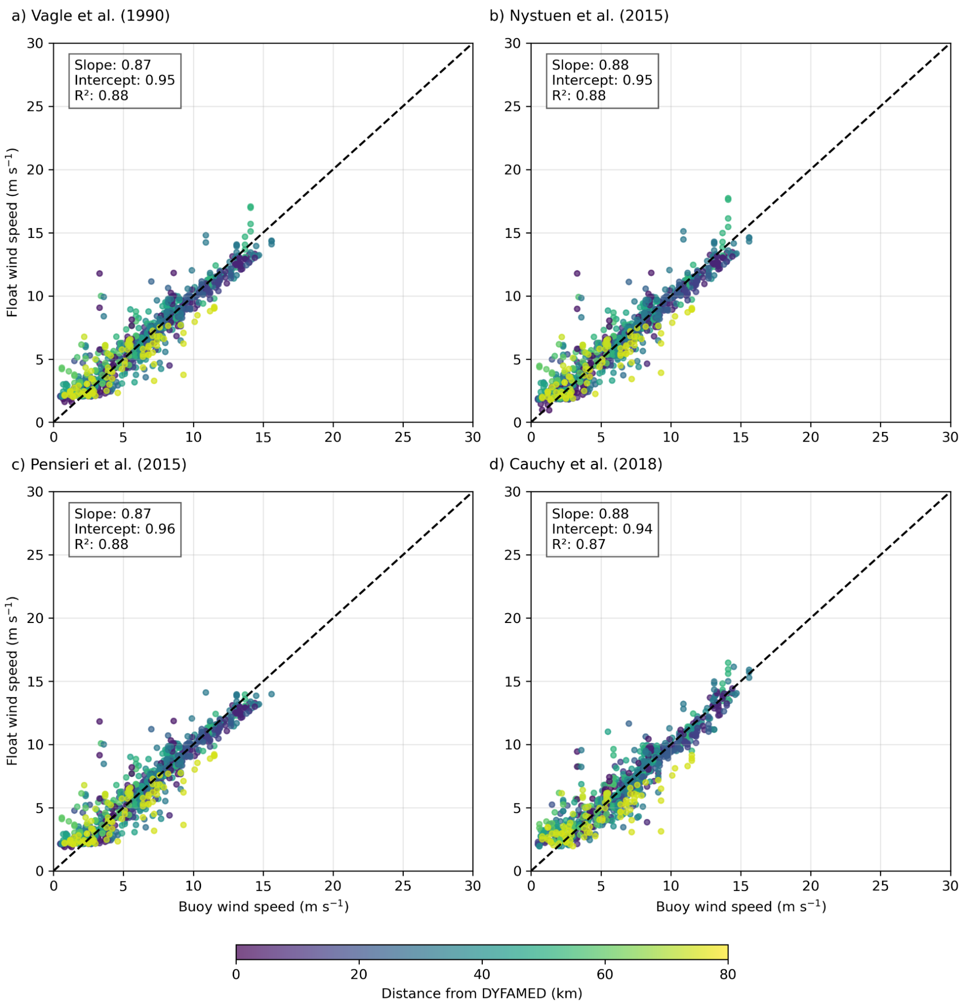

Figure 5. Comparison of optimised wind speed estimates from four literature models against collocated DYFAMED buoy wind measurements. Each subplot (a–d) shows scatter plots of float-derived wind speed vs. buoy wind speed using model-specific optimised coefficients: (a) Vagle et al. (1990), (b) Nystuen et al. (2015), (c) Pensieri et al. (2015), and (d) Cauchy et al. (2018). Points are color-coded by distance from the DYFAMED buoy, and the dashed line represents the 1:1 reference. Insets display linear regression slope, intercept, and coefficient of determination (R^2).

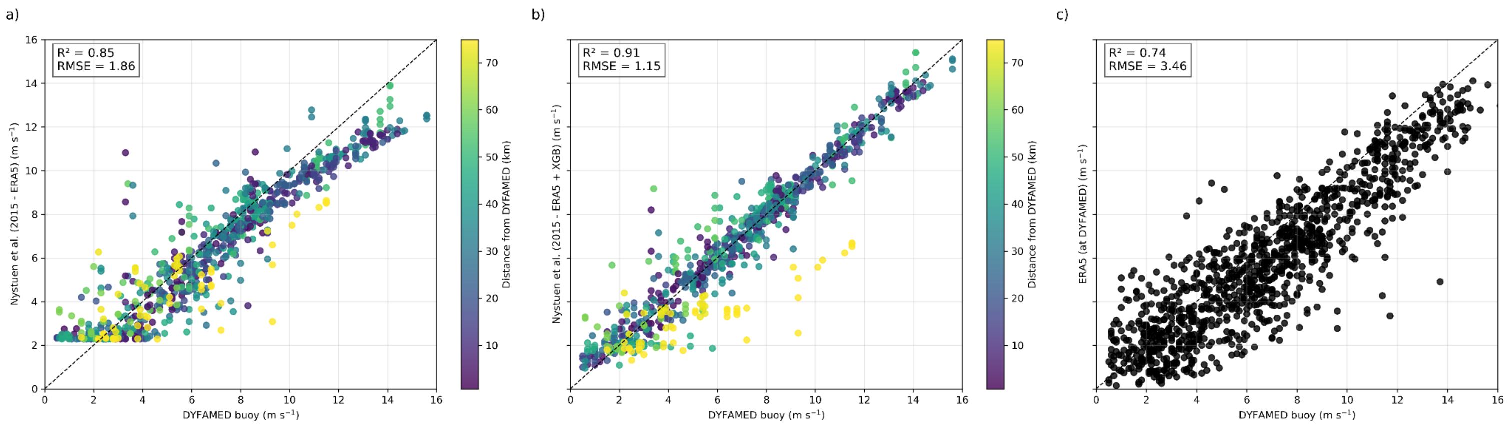

Figure 6. Comparison between DYFAMED buoy wind speed measurements and float-derived estimates using the Nystuen et al. (2015) acoustic model: (a) wind speeds estimated using Nystuen's polynomial formulation fit to ERA5; (b) same model corrected using a residual-learning approach with XGBoost, trained on the differences between ERA5-based estimates and DYFAMED observations; and (c) ERA5 wind speed at the DYFAMED grid point compared directly to buoy measurements for February, March and April 2025. Each point is colored by the float's distance from DYFAMED in panels (a) and (b). Dashed lines denote 1:1 agreement. All wind speeds are expressed in meters per second ($m\ s^{-1}$).

https://doi.org/10.5194/egusphere-2025-4174
Preprint. Discussion started: 14 October 2025

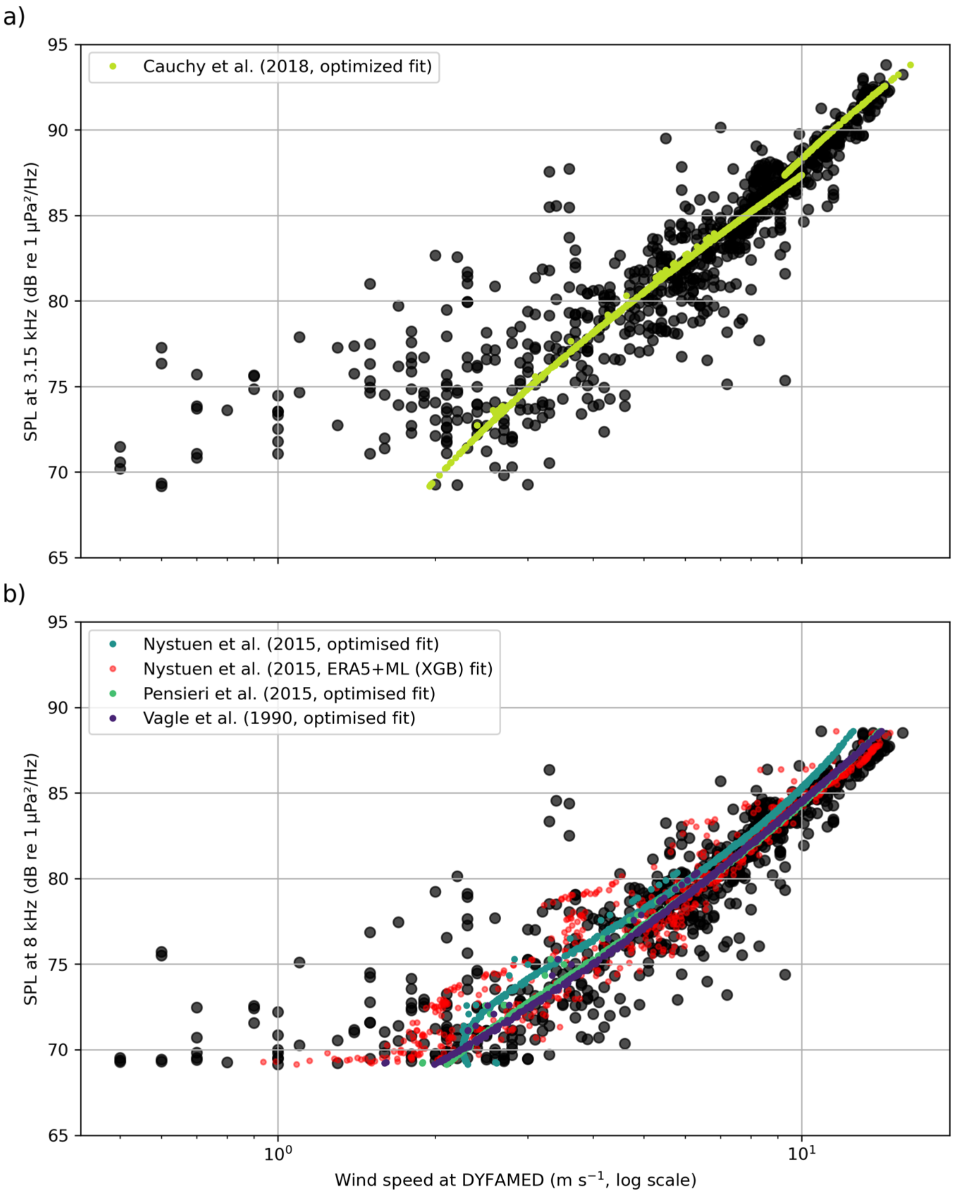

Figure 7. Optimised 10-meter wind speed (log scale) as a function of observed underwater sound pressure level (SPL) at DYFAMED for (a) 3.15 kHz and (b) 8 kHz. Observed wind speed is shown in black.

https://doi.org/10.5194/egusphere-2025-4174
Preprint. Discussion started: 14 October 2025

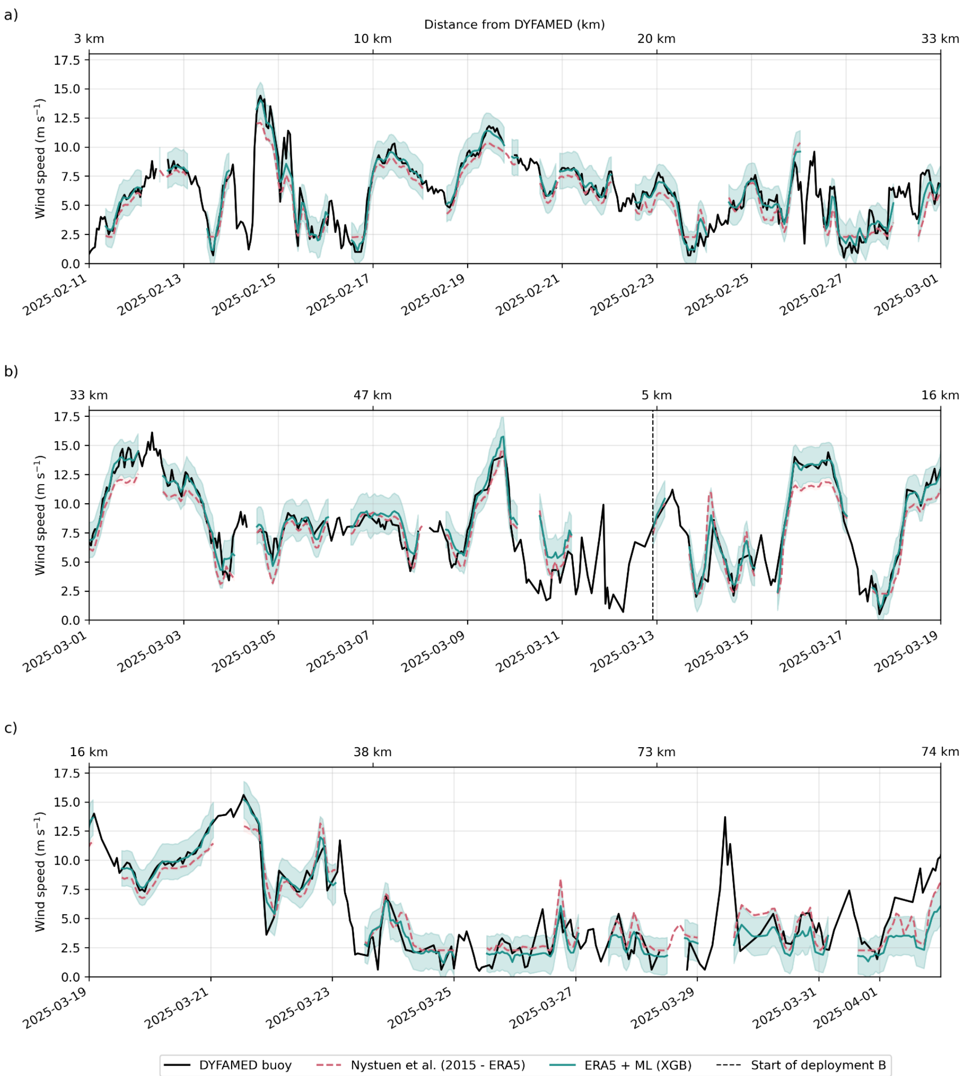

Figure 8. Time series comparison of wind speed estimates from the acoustic float and DYFAMED buoy observations, shown across three sequential 18-day segments of the deployment (a–c). The dashed pink line shows estimates from the Nystuen et al. (2015) model fit to ERA5-derived inputs. The solid green line represents the same model corrected using a residual-learning approach (XGBoost) with its associated uncertainty. Black curves show in-situ wind speed from the DYFAMED buoy. The top x-axis indicates the float's distance from DYFAMED over time, and a dashed vertical line marks the start of deployment B.

https://doi.org/10.5194/egusphere-2025-4174
Preprint. Discussion started: 14 October 2025

3.1 Assessing the performance of float-based acoustic wind estimation

We applied four previously published wind retrieval models to float-measured sound pressure levels (SPLs) at 8 kHz and 3 kHz. Using the original coefficients from these studies, wind speed estimates deviated significantly from collocated DYFAMED observations, particularly in their ability to reproduce the magnitude of wind events (Fig. 4a). This mismatch reflects the sensitivity of empirical acoustic models to deployment context, including platform geometry, acoustic propagation, and local noise environment.

When these same models were refitted using collocated float acoustics and DYFAMED wind observations within 40 km (Fig. 1), performance improved markedly (Fig. 4b; Fig. 7). Among the models, the cubic formulation by Nystuen et al. (2015) achieved the best fit ($R^2 = 0.88$; Fig. 5b) and successfully captured the full observed wind range (0.5–16.1 m s^{-1}; Figs. 5 and 7). Notably, it was the only model capable of resolving wind speeds below 2 m s^{-1}, a critical range often underrepresented due to weak surface forcing and minimal bubble generation. This low-end sensitivity is particularly valuable for air–sea gas exchange estimates in biogeochemical studies and suggests that the Nystuen model may be more broadly applicable in low-to-moderate wind regimes.

However, even after successful fitting, the transferability of acoustic–wind models remains uncertain. Factors such as noise contamination, ambient biological activity and regional propagation conditions can vary substantially between deployments, affecting both the shape and robustness of the acoustic–wind relationship. Moreover, profiling floats introduce their own artifacts, which may arise from hydrodynamic turbulence, buoyancy engine activity, bubble release, or electronic interference, each of which can contaminate the acoustic signal independently of wind forcing. In our study, even models originally developed in the same basin required refitting (i.e. Pensieri et al. 2015; Figs. 4, 5 and 7), underlining the challenge of cross-platform and cross-region generalization.

A promising future direction may involve grouping deployments into broader "acoustic environment types"—such as open-ocean gyres, coastal shelves, or high-latitude storm zones—within which shared model parameters could be defined and validated. This aligns with the priorities outlined in the Ocean Sound Essential Ocean Variable (EOV) Implementation Plan, which emphasizes the need for community-agreed metadata standards, calibration protocols, and classification schemes to support global comparability across acoustic deployments (Tyack et al., 2023). Evaluating the adequacy of such frameworks in the context of profiling float–based wind retrieval could inform future updates and promote harmonization with broader ocean observing efforts.

3.2 Generalizing float-specific wind modelling using reanalysis

While site-specific fitting of acoustic wind models yields accurate float-derived wind estimates, such fittings are not feasible in most regions of the global ocean where in-situ wind observations are unavailable. To assess whether the acoustic–wind relationship can be

https://doi.org/10.5194/egusphere-2025-4174
Preprint. Discussion started: 14 October 2025

generalized for remote deployments, we investigated the use of reanalysis wind products as a proxy reference for model fitting. Specifically, we used the ERA5 atmospheric reanalysis (Bell et al., 2021) to refit the Nystuen et al. (2015) model to float-measured acoustic data, simulating a scenario where no collocated buoy or shipboard wind measurements are available (Figs. 6 and 8).

Using time-matched float sound pressure level at 8 kHz and collocated ERA5 wind speed, we derived a new set of coefficients (Section 2.6), representing a general-purpose acoustic wind model that could, in principle, be deployed globally using only float data and reanalysis inputs. The objective of this exercise was not to develop a new region-specific model, but rather to test whether existing models could be adapted—via reanalysis fitting—for use in data-sparse areas, ultimately enabling scalable wind estimation from profiling floats globally.

As shown in Figure 6a, this ERA5-calibrated Nystuen et al. (2015) model reproduced wind variability within the 2.5–10 m s^{-1} range with moderate skill ($R^2 = 0.85$), and performed best during Deployment A, when wind conditions remained relatively stable and within the moderate wind regime (Fig. 8). However, performance declined during periods of stronger wind, particularly in Deployment B (Figs. 6a and 8). In these cases, the model systematically underestimated wind speeds, with errors exceeding 3 m s^{-1} during high-wind events.

Comparison with ERA5 reanalysis also revealed broader limitations. Although ERA5 provides a globally consistent reference product for surface winds, it diverged from DYFAMED data during several high-wind episodes, especially in Deployment B. This discrepancy is consistent with earlier studies reporting the underestimation of localized orographic wind events in reanalysis datasets over semi-enclosed basins such as the Mediterranean (Bentamy et al., 2003; Bell et al., 2021). This limitation is especially consequential for deployments in the Southern Ocean, where high-wind regimes are frequent and drive a large share of the global air–sea CO_2 flux. Underestimating these events could lead to significant biases, as gas exchange scales nonlinearly with wind speed (Wanninkhof, 2014; Wanninkhof et al., 2025).

Thus, while float-based acoustic wind estimation can be extended using reanalysis data in the absence of in-situ observations, its accuracy ultimately depends on the fidelity of the reference product used for fitting. In our case, reanalysis-based fitting performed well in moderate wind regimes but failed to capture the intensity of high-wind events—highlighting the limitations of relying solely on global reanalysis in dynamic or orographically complex regions.

3.3 Simulating scalable wind estimation in data-sparse regions

While reanalysis-calibrated acoustic models offer a pathway for estimating surface wind speed in remote regions, the results in Section 3.2 show that this approach alone remains insufficient during high-wind events or rapidly evolving conditions. This limitation poses a significant challenge for air–sea interaction studies in the Southern Ocean and other high-

https://doi.org/10.5194/egusphere-2025-4174
Preprint. Discussion started: 14 October 2025

latitude regions, where extreme wind forcing drives critical fluxes of heat, momentum, and carbon (Lee et al., 2017; Dotto et al., 2019; Zhang et al., 2022; Gruber et al., 2023).

3.3.1 Local model correction using residuals learning

To overcome this, we implemented a residual learning framework that combines the generalizability of reanalysis-based fitting with the accuracy of localized corrections. Specifically, we trained an ensemble of XGBoost regression models to predict the residuals between the ERA5-calibrated estimates and collocated DYFAMED buoy observations (see Section 2.6). The model was trained using float data within 40 km of DYFAMED and bootstrapped over 100 iterations to estimate both mean corrections and predictive uncertainty (Fig. 1; Fig. 6b). The 40 km radius was selected based on the sensitivity analysis of Cauchy et al. (2018), who found it to balance proximity with data availability; however, this threshold may be site-specific and should be re-evaluated in future deployments to reflect local acoustic and meteorological conditions.

The corrected wind time series showed markedly improved alignment with DYFAMED observations (Fig. 8), particularly during high-wind events where the uncorrected model consistently underestimated wind speed. This bias-correction approach yielded a substantial performance gain, increasing the coefficient of determination (R^2) from 0.85 to 0.91—an absolute improvement of 0.06, or approximately 7.1% relative to the baseline model. At the same time, the root mean square error (RMSE) dropped from 1.88 m s^{-1} to 1.15 m s^{-1}, corresponding to a 37.0% reduction in prediction error. While other learning-based methods have achieved comparable improvements—e.g., Zambra et al. (2022) reported a 16% RMSE reduction using a physics-informed deep learning model—our method differs by explicitly using reanalysis as a prior and requiring only sparse in-situ fitting.

The machine learning model does not estimate wind speed directly. Instead, it learns to adjust the bias based on a limited number of input features: acoustic signal intensity, deployment day, and the ERA5-calibrated prediction. In essence, it identifies when and where ERA5 is likely to fail, applying larger corrections under high-wind conditions where reanalysis tends to underestimate variability.

The results demonstrate that even a limited number of in-situ fitting points—simulating, for example, a brief engine-off ship-based wind measurement window during float deployment—could significantly improve wind estimates across the full float trajectory. In our case, the in-situ data used for fitting represented approximately 40% of the full dataset, due to the relatively short deployment duration. However, this approach also introduces potential limitations. First, although we aimed to simulate operational constraints, the fitting points were drawn from the same dataset used for evaluation, raising the possibility of optimistic bias in the reported performance. Future deployments should explore spatially or temporally distinct training–validation splits or assess generalization using fully withheld reference stations. Second, the observed reduction in RMSE reflects improvements primarily at the higher end of the wind

https://doi.org/10.5194/egusphere-2025-4174
Preprint. Discussion started: 14 October 2025

speed range, where raw model errors tend to be largest. While this benefits absolute RMSE metrics, it may overstate improvements at lower wind speeds.

3.3.2 Strategies for sparse in-situ calibration

In practical terms, however, acquiring suitable reference observations can be challenging. While ship-based wind measurements are a natural candidate—particularly during float deployment or recovery—they may be unsuitable for model fitting if the ship is too close, as engine noise can contaminate the float's acoustic signal. A viable compromise is to position the ship nearby—but not too close—so that wind speed measurements remain representative while minimizing acoustic interference. Alternatively, a more robust strategy is to deploy floats in proximity to existing meteorological buoys, which provide collocated wind observations without interfering with subsurface acoustic recordings.

In regions where neither buoys nor suitable ship data are available, identifying whether the available in-situ coverage is sufficient becomes more complex. This will depend not only on the duration and trajectory of the float mission, but also on the opportunistic use of additional reference sources encountered along the way—for example, other buoys, or wind observations from vessels transiting the area. In such cases, satellite-based products—particularly synthetic aperture radar (SAR) imagery—could offer another valuable source of wind information. These products provide high spatial resolution and can capture localized wind variability at times and locations where in-situ data are sparse. Although episodic and weather-dependent, SAR passes could serve as intermittent anchor points for model adjustment or evaluation.

More broadly, these scenarios highlight the need for flexible modelling approaches that can exploit heterogeneous and temporally limited reference data. Rather than relying on dense training datasets or persistent surface observations, future efforts could explore machine learning paradigms such as domain adaptation, transfer learning, or few-shot learning, which aim to adapt models to new environments with minimal retraining. For instance, recent work by Wang et al. (2020) has shown that few-shot transfer methods can yield competitive performance even when only a small number of target-domain samples are available.

In the context of profiling floats, such strategies could enable a more scalable approach to acoustic model tuning, by leveraging sparse data from ships, buoys, or satellites—each with its own limitations but collectively offering sufficient diversity. We propose framing this as opportunistic multisource model fine-tuning: a hybrid calibration scheme in which local corrections are derived from whatever reference sources are available, without requiring dense or continuous in-situ coverage. Developing and validating such methods will be essential to deploy acoustic-equipped floats globally while maintaining robustness across a wide range of environmental and acoustic conditions.

https://doi.org/10.5194/egusphere-2025-4174
Preprint. Discussion started: 14 October 2025

3.3.3 Implications for global observing

While ERA5 provides a useful climatological reference, it tends to underestimate short-lived, high-wind events due to spatial and temporal smoothing. This is an issue particularly for gas exchange studies, as extreme winds disproportionately contribute to total fluxes. Acoustic float data—collected continuously and at high resolution—are uniquely positioned to detect these events, even when they fall below the detection threshold of satellite or reanalysis products.

However, model performance degrades with increasing distance from DYFAMED, reflecting the spatial decorrelation of wind fields and the limited spatial representativeness of the buoy observations. Beyond 73 km during Deployment B, both the Nystuen et al. (2015) – ERA5 fit and the machine-learning-corrected float estimates begin to diverge from DYFAMED winds (Figs. 6 and Fig. 8). This divergence does not necessarily imply model failure but rather raises the possibility that the float and buoy are sampling different wind regimes. In such cases, it becomes difficult to determine whether discrepancies are due to limitations in the acoustic model or to true spatial variability in wind forcing. One way to address this uncertainty is to analyse float trajectories that pass between two surface reference stations, assessing whether refitting at the final station yields consistent corrections or reveals systematic regional shifts in wind decorrelation. Such an approach will require future deployments that span multiple buoys, enabling a systematic evaluation of how model performance degrades—or remains robust—across both time and space.

Additionally, in the Southern Ocean, where anthropogenic noise is relatively low, it may also be worth reconsidering the use of lower-frequency bands (<1 kHz) for wind estimation. These frequencies are more sensitive to high wind speeds due to increased bubble activity and longer propagation ranges and may outperform higher-frequency bands under strong forcing conditions—provided contamination from distant shipping or other sources remains minimal.

Several recent studies have applied machine learning to underwater acoustic data to estimate wind and rainfall, often relying on long-term, stationary deployments and direct prediction from spectral features (Taylor et al., 2020; Trucco et al., 2022; Trucco et al., 2023; Zambra et al., 2022). While these approaches have shown strong performance under controlled conditions—such as Taylor et al.'s use of moored PAL systems during storm events or Zambra et al.'s assimilation-based deep learning scheme—they typically require dense, labelled datasets and assume relatively stable acoustic environments.

In contrast, our residual learning strategy is designed for sparse, mobile deployments. It corrects reanalysis-based estimates using short-duration in-situ fitting and does not require full acoustic training labels, making it more adaptable to the practical constraints of autonomous profiling floats. While in-situ data remains the most difficult to obtain in remote, data-poor regions, our approach is well-suited to opportunistic fitting—for instance, using brief ship-based wind observations during deployment or leveraging nearby meteorological buoys. This hybrid strategy balances scalability with realism, enabling robust performance even in hard-to-access areas where long-term reference data are limited or unavailable.

https://doi.org/10.5194/egusphere-2025-4174
Preprint. Discussion started: 14 October 2025

In parallel, another important consideration is the potential for regional bias introduced by the depth correction applied to acoustic levels. This correction compensates for propagation losses due to local water column properties (e.g., temperature, salinity, and sound speed) and is typically derived from the float's hydrographic profile at the start of the deployment. When used to adjust the full acoustic time series, this introduces a location-dependent correction that may vary across floats or missions. Ideally, the correction should be recalculated for each new hydrographic profile, especially in long-term or wide-ranging deployments where temperature and salinity conditions evolve. To ensure comparability of wind estimates at basin or global scales, such corrections should be clearly documented and incorporated into standard processing protocols for acoustic-equipped floats.

This deployment-focused flexibility is key to scaling up acoustic wind estimation globally. By leveraging reanalysis products for first order fitting and applying localized corrections when available, our framework enables accurate, event-resolving wind estimates without the need for long-term surface infrastructure. Scaling this approach across the BGC-Argo array would provide high-resolution, all-weather wind monitoring in regions poorly served by existing networks.

4 Conclusions

This study provides the first demonstration of retrieving surface wind speeds from subsurface ambient noise recorded by a profiling float equipped with a passive acoustic sensor. By integrating a low-power hydrophone onto an autonomous profiling float and applying established acoustic retrieval algorithms, we successfully detected surface wind variability from depths between 500 and 1000 m. When empirically calibrated using collocated buoy observations, float-derived wind speed estimates closely matched in-situ surface measurements, confirming the feasibility and accuracy of this approach under realistic oceanographic conditions.

To evaluate its potential for application in remote, data-sparse regions, we simulated a scenario where acoustic models were calibrated solely using ERA5 reanalysis winds. Although the ERA5-based calibration captured moderate wind variability effectively (2.5–10 m s^{-1}), it consistently underestimated high-wind events, underscoring limitations in using reanalysis data as a standalone reference. To mitigate this, we implemented a residual-learning approach, leveraging brief periods of local wind observations (e.g., from ship-based or moored instruments) to correct systematic errors in the acoustic estimates. This hybrid methodology substantially improved model performance, particularly under high-wind conditions, maintaining accuracy across extended float trajectories and demonstrating robustness for operational use.

These findings underscore the potential of acoustic-equipped profiling floats as scalable and autonomous platforms capable of delivering high-resolution surface wind observations in remote or poorly instrumented oceanic regions. Such observations are particularly critical for

https://doi.org/10.5194/egusphere-2025-4174
Preprint. Discussion started: 14 October 2025

refining estimates of air–sea exchanges, including the oceanic uptake and release of CO_2, processes significantly influenced by wind-driven gas exchange. Combined with emerging biogeochemical proxy algorithms, such as CANYON-B and CONTENT, acoustic-equipped floats can now provide fully autonomous, integrated estimates of air–sea CO_2 fluxes by coupling accurate wind measurements with concurrent measurements of oceanic temperature, salinity, and oxygen.

Nevertheless, this study represents a single deployment in a semi-enclosed basin. Broader validation across diverse oceanographic regimes, including open-ocean gyres, polar regions, and high-energy storm zones, is necessary to fully assess the robustness, generalizability, and temporal stability of the proposed correction frameworks. Future deployments will help refine the methods presented here and further test their applicability across different acoustic environments and platform configurations.

The demonstrated capability to retrieve accurate wind speeds from subsurface acoustic measurements marks a significant advancement in autonomous ocean observing. As next-generation passive acoustic sensors become increasingly integrated into the global BGC-Argo array, this technology offers a cost-effective and efficient strategy for addressing persistent observational gaps. Such developments will enable unprecedented insights into wind forcing, air–sea interactions, and climate-relevant ocean processes in regions historically challenging to monitor through traditional methods.

Looking forward, the ability to calibrate acoustic wind retrievals using sparse local reference measurements not only improves float-based wind estimates but also provides a valuable new data stream for validating and potentially correcting biases in global wind reanalyses. As acoustic-equipped floats accumulate data across various ocean regions, their observations may substantially enhance the fidelity of global atmospheric products, particularly in remote areas currently lacking validation data.

Ultimately, this work aligns closely with the Ocean Sound Essential Ocean Variable (EOV) Implementation Plan, advocating for standardized methodologies, robust metadata documentation, and interoperable frameworks across acoustic observing platforms. Demonstrating successful acoustic wind retrieval from autonomous, mobile platforms thus contributes directly to the practical realization of global observing standards, strengthening the integration of passive acoustics into sustained, multidisciplinary ocean observing systems.

https://doi.org/10.5194/egusphere-2025-4174
Preprint. Discussion started: 14 October 2025

Funding. The research leading to these results has received part of the funding from the European Union's Horizon research and innovation program under grants #101094716 (GEORGE project) and #101188028 (TRICUSO project). REFINE has received funding from the European Research Council (ERC) under the European Union's Horizon 2020 research and innovation programme (grant agreement N° 834177). Argo-2030 has received the support of the French government within the framework of the "Investissements d'avenir" program integrated in France 2030 and managed by the Agence Nationale de la Recherche (ANR) under the reference "ANR-21-ESRE-0019".

Data availability. The two deployments of this prototype float have not been assigned a WMO identifier and have not been declared in Argo; the data are therefore not available through the Argo program. All float data, DYFAMED buoy measurements, ERA5 reanalysis wind fields, and analysis scripts used in this study is freely available online at https://doi.org/10.5281/zenodo.17232551.The repository include processed datasets, code for model fitting and residual learning, and figure-generation scripts to ensure full reproducibility of results.

Author contributions. EL, HC, and LD conceptualized the project. AD and CS developed the acoustic sensor used in this study. LD curated the data. EL, HC, and LD performed the investigation. LD conceptualized the methodology, used the necessary software, visualized the data, and prepared the original draft of the paper. AGM, DC, EL, HC, JB, LD, PC, RB and SP reviewed and edited the paper.

Competing interests. NKE instrumentation is a private company which commercialized the acoustic float, in which AD and CS are employed. The acoustic float is based on the PROVOR CTS5 platform and on an acoustic sensor developed and commercialized by NKE instrumentation with a partnership agreement with LOV. All other co-authors declare no competing interests.

Disclaimer. Publisher's note: Copernicus Publications remains neutral with regard to jurisdictional claims in published maps and institutional affiliations.

Acknowledgements. We gratefully acknowledge the DYFAMED team at the Laboratoire d'Océanographie de Villefranche for their support in deploying the float, recovering it, and enabling its second deployment. We also thank the crew of the Téthys for their assistance at sea, and Jean-Yves for facilitating two successful float recoveries on short notice. We are grateful to the European Centre for Medium-Range Weather Forecasts (ECMWF) for making the ERA5 reanalysis products freely available, which provided an essential reference dataset for this study. We also thank Aldo Napoli (Mines Paris) for his assistance with the AIS data and Ambroise Renaud (Mines Paris) for making his modified version of *libais* freely available on GitHub, which allowed us to parse NMEA data from the AIS reception device at Mines Paris (Sophia Antipolis) and from the AISHub feed. We are also grateful to AISHub (AIS data sharing and vessel tracking by AISHub) for providing access to their AIS data services.

References

Anagnostou, E. N., Nystuen, J. A., and Papadopoulos, A. (2001). Listening to raindrops from underwater: an acoustic disdrometer. Journal of Atmospheric and Oceanic Technology, 18(10), 1640–1657.

Baumgartner, M. F., Stafford, K. M., and Latha, G. (2017). Near real-time underwater passive acoustic monitoring of natural and anthropogenic sounds. In Observing the Oceans in Real Time (pp. 203–226).

Baumgartner, M. F., and Bonnel, J. (2022, March). Real-time detection and classification of marine mammals from expendable profiling floats. In Workshop on Detection, Classification, Localization and Density Estimation of Marine Mammals using Passive Acoustics, Oahu, USA.

Bell, B., Hersbach, H., Simmons, A., Berrisford, P., Dahlgren, P., Horányi, A., Muñoz-Sabater, J., Nicolas, J., Radu, R., Schepers, D., ... and Thépaut, J.-N. (2021). The ERA5 global reanalysis: Preliminary extension to 1950. Quarterly Journal of the Royal Meteorological Society, 147(741), 4186–4227. https://doi.org/10.1002/qj.4174

Bentamy, A., Katsaros, K. B., Mestas-Nuñez, A. M., Drennan, W. M., Forde, E. B., and Roquet, H. (2003). Satellite estimates of wind speed and latent heat flux over the global oceans. Journal of Climate, 16(4), 637–656.

Bittig, H. C., Steinhoff, T., Claustre, H., Fiedler, B., Williams, N. L., Sauzède, R., Körtzinger, A., and Gattuso, J.-P. (2018). Robust estimation of open ocean CO_2 variables and nutrient concentrations using Bayesian neural networks. Frontiers in Marine Science, 5, 328.

Bushinsky, S. M., Gray, A. R., Johnson, K. S., and Sarmiento, J. L. (2017). Oxygen in the Southern Ocean from Argo floats: Determination of processes driving air-sea fluxes. Journal of Geophysical Research: Oceans, 122(11), 8661–8682.

Carranza, M. M., Long, M. C., Di Luca, A., et al. (2024). Extratropical storms induce carbon outgassing over the Southern Ocean. npj Climate and Atmospheric Science, 7, 106. https://doi.org/10.1038/s41612-024-00657-7

Cauchy, P., Heywood, K. J., Merchant, N. D., Queste, B. Y., and Testor, P. (2018). Wind speed measured from underwater gliders using passive acoustics. Journal of Atmospheric and Oceanic Technology, 35(12), 2305–2321. https://doi.org/10.1175/JTECH-D-17-0209.1

Cazau, D., Bonnel, J., and Baumgartner, M. (2018). Wind speed estimation using an acoustic underwater glider in a near-shore marine environment. IEEE Transactions on Geoscience and Remote Sensing, 57(4), 2097–2106.

Cazau, D., Bonnel, J., Jouma'a, J., Le Bras, Y., and Guinet, C. (2017). Measuring the marine soundscape of the Indian Ocean with southern elephant seals used as acoustic gliders of opportunity. Journal of Atmospheric and Oceanic Technology, 34(2), 207–223. https://doi.org/10.1175/JTECH-D-16-0124.1

Chelton, D. B., Schlax, M. G., Samelson, R. M., and de Szoeke, R. A. (2007). Global observations of large oceanic eddies. Geophysical Research Letters, 34(15). https://doi.org/10.1029/2007GL030812

Chen, T., and Guestrin, C. (2016). XGBoost: A scalable tree boosting system. In Proceedings of the 22nd ACM SIGKDD International Conference on Knowledge Discovery and Data Mining (KDD '16), pp. 785–794. https://doi.org/10.1145/2939672.2939785

Claustre, H., Johnson, K. S., and Takeshita, Y. (2020). Observing the global ocean with Biogeochemical-Argo. Annual Review of Marine Science, 12, 23–48.

D'ortenzio, F., Taillandier, V., Claustre, H., et al. (2020). Biogeochemical Argo: The test case of the NAOS Mediterranean array. Frontiers in Marine Science, 7, 120.

Dotto, T. S., Naveira Garabato, A. C., Bacon, S., et al. (2019). Wind-driven processes controlling oceanic heat delivery to the Amundsen Sea, Antarctica. Journal of Physical Oceanography, 49(11), 2829–2849.

Farahani, A., Voghoei, S., Rasheed, K., and Arabnia, H. R. (2020). A brief review of domain adaptation. arXiv preprint arXiv:2010.03978. https://arxiv.org/abs/2010.03978

Farmer, D. M., Vagle, S., and Booth, A. D. (1998). A free-flooding acoustical resonator for measurement of bubble size distributions. Journal of Atmospheric and Oceanic Technology, 15(5), 1132–1146.

Fregosi S, Harris DV, Matsumoto H, Mellinger DK, Barlow J, Baumann-Pickering S and Klinck H (2020) Detections of Whale Vocalizations by Simultaneously Deployed Bottom-Moored and Deep-Water Mobile Autonomous Hydrophones. Front. Mar. Sci. 7:721. doi: 10.3389/fmars.2020.00721.

Gray, A. R., Johnson, K. S., Bushinsky, S. M., et al. (2018). Autonomous biogeochemical floats detect significant carbon dioxide outgassing in the high-latitude Southern Ocean. Geophysical Research Letters, 45(17), 9049–9057.

Gros-Martial, A., Dubus, G., Cazau, D., Bazin, S., and Guinet, C. (2025). Producing a new in-situ wind speed product for the Southern Ocean based on acoustic meteorology from biologged southern elephant seals. Journal of Atmospheric and Oceanic Technology. https://doi.org/10.1175/JTECH-D-25-0037.1

Gruber, N., Bakker, D. C. E., DeVries, T., et al. (2023). Trends and variability in the ocean carbon sink. Nature Reviews Earth and Environment, 4(2), 119–134. https://doi.org/10.1038/s43017-022-00381-x

Johnson, K., and Claustre, H. (2016). Bringing biogeochemistry into the Argo age. Eos, Transactions American Geophysical Union.

Johnson, K. S., Riser, S. C., and Karl, D. M. (2010). Nitrate supply from deep to near-surface waters of the North Pacific subtropical gyre. Nature, 465(7301), 1062–1065.

Li, Z., Thompson, E. J., Behrangi, A., Chen, H., and Yang, J. (2023). Performance of GPCP daily products over oceans: Evaluation using Passive Aquatic Listeners. Geophysical Research Letters, 50, e2023GL104310. https://doi.org/10.1029/2023GL104310

Ma, B. B., Girton, J. B., Dunlap, J. H., Gobat, J. I., and Chen, J. (2023). Passive acoustic measurements on autonomous profiling floats. OCEANS 2023 - MTS/IEEE U.S. Gulf Coast, 1–6. https://doi.org/10.23919/OCEANS52994.2023.10337032

Ma, B. B., and Nystuen, J. A. (2005). Prediction of underwater sound levels from rain and wind. Journal of the Acoustical Society of America, 117(6), 3555–3565. https://doi.org/10.1121/1.1910283

Matsumoto, H., Jones, C., Klinck, H., et al. (2013). Tracking beaked whales with a passive acoustic profiler float. Journal of the Acoustical Society of America, 133(2), 731–740.

McGillicuddy Jr, D. J. (2016). Mechanisms of physical-biological-biogeochemical interaction at the oceanic mesoscale. Annual Review of Marine Science, 8(1), 125–159.

McMonigal, K., Larson, S. M., and Gervais, M. (2025). Wind-Driven Ocean Circulation Changes Can Amplify Future Cooling of the North Atlantic Warming Hole. Journal of Climate, 38(11), 2479-2496.

Menze, S., Kindermann, L., van Opzeeland, I., et al. (2013). Soundscapes of the Southern Ocean: Passive acoustic monitoring in the Weddell Sea. [Conference Presentation].

Nystuen, J. A., Anagnostou, M. N., Anagnostou, E. N., and Papadopoulos, A. (2015). Monitoring Greek seas using passive underwater acoustics. Journal of Atmospheric and Oceanic Technology, 32(2), 334–349.

Oguz, H. N., and Prosperetti, A. (1990). Bubble entrainment by the impact of drops on liquid surfaces. Journal of Fluid Mechanics, 219, 143–179.

Pensieri, S., Bozzano, R., Nystuen, J. A., et al. (2015). Underwater acoustic measurements to estimate wind and rainfall in the Mediterranean Sea. Advances in Meteorology, 2015, 612512. https://doi.org/10.1155/2015/612512

Pipatprathanporn, S., and Simons, F. J. (2022). One year of sound recorded by a MERMAID float in the Pacific: Hydroacoustic earthquake signals and infrasonic ambient noise. Geophysical Journal International, 228(1), 193–212.

Prawirasasra, M. S., Mustonen, M., Klauson, A. 2024. Wind fetch effect on underwater wind-driven sound. Estonian Journal of Earth Sciences, 73(1), 15–25. https://doi.org/10.3176/earth.2024.02

Rainaud, R., et al. (2016). Characterization of air–sea exchanges over the Western Mediterranean Sea during HyMeX SOP1 using the AROME–WMED model. Quarterly Journal of the Royal Meteorological Society, 142, 173–187. https://doi.org/10.1002/qj.2480

Riser, S. C., Nystuen, J., and Rogers, A. (2008). Monsoon effects in the Bay of Bengal inferred from profiling float-based measurements of wind speed and rainfall. Limnology and Oceanography, 53(5), 2080–2093. https://doi.org/10.4319/lo.2008.53.5_part_2.2080

Taylor, W. O., Anagnostou, M. N., Cerrai, D., and Anagnostou, E. N. (2021). Machine learning methods to approximate rainfall and wind from acoustic underwater measurements. IEEE Transactions on Geoscience and Remote Sensing, 59(4), 2810–2821. https://doi.org/10.1109/TGRS.2020.3007557

Trucco, A., Barla, A., Bozzano, R., et al. (2022). Compounding approaches for wind prediction from underwater noise by supervised learning. IEEE Journal of Oceanic Engineering, 47(4), 1172–1187.

Trucco, A., Barla, A., Bozzano, R., et al. (2023). Introducing temporal correlation in rainfall and wind prediction from underwater noise. IEEE Journal of Oceanic Engineering, 48(2), 349–364. https://doi.org/10.1109/JOE.2022.3223406

Vagle, S., Large, W. G., and Farmer, D. M. (1990). An evaluation of the WOTAN technique of inferring oceanic winds from underwater ambient sound. Journal of Atmospheric and Oceanic Technology, 7(4), 576–595.

Verhoef, A., Portabella, M., and Stoffelen, A. (2012). High-resolution ASCAT scatterometer winds near the coast. IEEE Transactions on Geoscience and Remote Sensing, 50(7), 2481–2487.

Wang, Y., Yao, Q., Kwok, J. T., and Ni, L. M. (2020). Generalizing from a few examples: A survey on few-shot learning. ACM computing surveys (csur), 53(3), 1-34.

Wanninkhof, R. (2014). Relationship between wind speed and gas exchange over the ocean revisited. Limnology and Oceanography: Methods, 12(6), 351–362. https://doi.org/10.4319/lom.2014.12.351

https://doi.org/10.5194/egusphere-2025-4174
Preprint. Discussion started: 14 October 2025

Wanninkhof, R., Triñanes, J., Pierrot, D., et al. (2025). Trends in sea-air CO_2 fluxes and sensitivities to atmospheric forcing using an extremely randomized trees machine learning approach. Global Biogeochemical Cycles, 39(2), e2024GB008315. https://doi.org/10.1029/2024GB008315

Williams, N. L., Juranek, L. W., Feely, R. A., et al. (2017). Calculating surface ocean pCO_2 from biogeochemical Argo floats equipped with pH: An uncertainty analysis. Global Biogeochemical Cycles, 31(3), 591–604. https://doi.org/10.1002/2016GB005541

Yang, J., Riser, S. C., Nystuen, J. A., Asher, W. E., and Jessup, A. T. (2015). Regional rainfall measurements: using the Passive Aquatic Listener during the SPURS field campaign. Oceanography, 28(1), 124–133.

Yang, J., Asher, W. E., and Riser, S. C. (2016, January). Rainfall measurements in the North Atlantic Ocean using underwater ambient sound. In 2016 IEEE/OES China Ocean Acoustics (COA) (pp. 1–4). IEEE.

Zambra, N., Lguensat, R., Pannekoucke, O., Fablet, R., and Chapron, B. (2022). 4DVarNet: End-to-end learning of variational data assimilation models. Machine Learning and Knowledge Extraction, 4(1), 1–20.

Zhang, M., Cheng, Y., Bao, Y., et al. (2022). Seasonal to decadal spatiotemporal variations of the global ocean carbon sink. Global Change Biology, 28(5), 1786–1797.